Four additional mouse crosses improve the lipid QTL landscape and identify *Lipg* as a QTL gene[S]

Zhiguang Su,* Naoki Ishimori,*,† Yaoyu Chen,* Edward H. Leiter,* Gary A. Churchill,* Beverly Paigen,* and Ioannis M. Stylianou[1,*,§]

The Jackson Laboratory,* Bar Harbor, ME 04609; Department of Cardiovascular Medicine,† Hokkaido University Graduate School of Medicine, Sapporo, Japan; and University of Pennsylvania,§ School of Medicine, Institute for Translational Medicine and Therapeutics, Philadelphia, PA 19104

Abstract To identify genes controlling plasma HDL and triglyceride levels, quantitative trait locus (QTL) analysis was performed in one backcross, (NZO/H1Lt × NON/LtJ) × NON/LtJ, and three intercrosses, C57BL/6J × DBA/2J, C57BL/6J × C3H/HeJ, and NZB/B1NJ × NZW/LacJ. HDL concentrations were affected by 25 QTL distributed on most chromosomes (Chrs); those on Chrs 1, 8, 12, and 16 were newly identified, and the remainder were replications of previously identified QTL. Triglyceride concentrations were controlled by nine loci; those on Chrs 1, 2, 3, 7, 16, and 18 were newly identified QTL, and the remainder were replications. Combining mouse crosses with haplotype analysis for the HDL QTL on Chr 18 reduced the list of candidates to six genes. Further expression analysis, sequencing, and quantitative complementation testing of these six genes identified *Lipg* as the HDL QTL gene on distal Chr 18. The data from these crosses further increase the ability to perform haplotype analyses that can lead to the identification of causal lipid genes.—Su, Z., N. Ishimori, Y. Chen, E. H. Leiter, G. A. Churchill, B. Paigen, and I. M. Stylianou. **Four additional mouse crosses improve the lipid QTL landscape and identify *Lipg* as a QTL gene. *J. Lipid Res.* 2009.** 50: **2083–2094.**

Supplementary key words high density lipoprotein • triglyceride • quantitative trait locus

Epidemiological studies show that high plasma triglyceride (TG) levels and low HDL cholesterol levels increase the risk of cardiovascular disease (1, 2). Raising HDL and lowering TG are therefore critical goals for coronary heart disease prevention. Two drug classes that raise HDL are available, fibrates and niacin; each has been shown to reduce the number of coronary events (3–9) even though they only modestly raise HDL, typically 5–20%. Furthermore, clinical use of niacin is limited due to a side effect of cutaneous flushing (10), while fibrates are associated with an increase in noncardiovascular mortality (11, 12). TG levels can be lowered through fibrates or omega-3 fatty acid treatment. Treatment with omega-3 fatty acids appears to reduce cardiovascular events (13, 14); however, other effects of treatment may contribute to the reduction of cardiovascular events since the decrease of TG is modest.

HDL levels vary considerably in humans, and this variation is at least 50% genetically determined (15). Several genes have been shown to contribute to the genetic variation of HDL in humans (16). With the advances in single nucleotide polymorphism (SNP) genotyping technology, genome-wide association studies have identified common variants in a small number of genes as being associated with human plasma lipid levels (17–26). For HDL, many of the significant SNPs have been reported in known genes, such as cholesterol ester transfer protein, hepatic lipase, lipoprotein lipase, ATP-binding cassette subfamily A member 1, lecithin cholesterol acyltransferase, and endothelial lipase. However, the effect sizes of the reported associations remain small, 5–10% cumulatively, suggesting that other genes and loci remain to be found.

Although quantitative trait loci (QTL) for lipids in animal models and humans have been extensively investigated, mouse QTL remain a required part of the genetic mapping toolbox, as modeling environmental effects in humans is challenging. Plasma HDL and TG levels vary among common strains of inbred mice, and numerous QTL for HDL have been mapped by crossing different strains (27, 28). While it is believed the HDL QTL map is

This work was funded by US National Institutes of Health grants to B.P. (HL-81162, HL-74086, and HL-77796) and GM-070683 to G.A.C., by American Heart Association Grant 0725905T to Z.S., and by the Novartis Institutes for Biomedical Research. Its contents are solely the responsibility of the authors and do not necessarily represent the official views of the National Institutes of Health.

Manuscript received 18 February 2009 and in revised form 8 May 2009.

Published, JLR Papers in Press, May 12, 2009
DOI 10.1194/jlr.M900076-JLR200

Abbreviations: Chr, chromosome; cM, centimorgan; QTL, quantitative trait locus; SNP, single nucleotide polymorphism; TC, total cholesterol; TG, triglyceride.

[1] To whom correspondence should be addressed.
e-mail: ist@mail.med.upenn.edu

[S] The online version of this article (available at http://www.jlr.org) contains supplementary data in the form of two figures and five tables.

approaching saturation with few new loci being reported (27), the additional crosses provide important information that can be used for combining data sets and haplotype analysis to further narrow loci and identify the genes (29). In comparison, few TG QTL have been reported, and the seven novel TG QTL reported here will likely aid the identification of TG QTL genes in the future as more crosses are performed.

This study reports plasma HDL and TG QTL from four new mouse crosses involving seven different strains. Furthermore, six additional HDL QTL crosses have been published since the last review (27) (**Table 1**). These separate crosses will aid haplotype analysis, and where possible, raw data from multiple crosses can be combined to narrow the QTL region and identify the underlying genes. In this study, some of the new QTL were used for combined-cross analysis with haplotype analysis, mRNA expression analysis, and quantitative complementation testing to identify and prove that endothelial lipase (*Lipg*) is an HDL quantitative trait gene on distal mouse chromosome (Chr) 18.

MATERIALS AND METHODS

Animals

C57BL/6J (B6), C3H/HeJ (C3H), DBA/2J (D2), NZO/HlLtJ (NZO), NON/LtJ (NON), NZB/B1NJ (NZB), and NZW/LacJ (NZW) inbred mouse strains and B6.129S-*Lipg*^{tm1Tq}/J (B6.*Lipg*$^{-/-}$, stock no. 005681) were obtained from The Jackson Laboratory. Mice were housed in a climate-controlled facility with a 12 h light/12 h dark cycle and allowed ad libitum access to water and a chow diet containing 6% fat (LabDiets 5K52; St. Louis, MO). Animal protocols were reviewed and approved by the Animal Care and Use Committee of The Jackson Laboratory.

Each cross, carried out for different reasons, is summarized here. B6 × D2 is a cross originally studied for albuminuria (30) phenotyped 335 chow-fed male F2 mice at 8 weeks of age. B6 × C3H, a cross with 277 female F2 mice generated from reciprocal mating, fed mice an atherogenic diet (Ath) as described previously from 8 to 14 weeks of age when they were phenotyped. (NZO × NON) × NON, a cross previously described for diabesity phenotypes (31), measured HDL and TG levels in 146 chow-fed males at 24 weeks of age. NZB × NZW, a cross with 264 F2 male and female mice, measured HDL and TG in mice fed the atherogenic diet from 8–16 weeks of age. TGs for this cross have been published previously (32).

Quantitative complementation testing was performed for *Lipg*. Male B6.*Lipg*$^{-/-}$ and B6 *Lipg*$^{+/+}$ mice were crossed with female B6, C3H, D2, NZB, or SM mice. Both sexes of the chow-fed F1 progeny from each mating were measured for HDL at 8 weeks of age.

Plasma lipid analysis

Crosses B6 × C3H and NZB × NZW were fasted for 4 h in the morning, while crosses for B6 × D2 and (NZO × NON) × NON were not fasted. Fasting does not usually affect HDL but may significantly alter TG levels, which could reduce the ability to identify TG QTL (false negatives) but should not create false positives. Thus, TG QTL are also reported for the unfasted crosses because they may be informative for future positional mapping of these QTL genes.

Blood from the retro-orbital sinus was collected in tubes containing EDTA and centrifuged at 9,000 rpm for 5 min. Plasma was frozen at –20°C until assay. Plasma HDL, total cholesterol (TC), and TG concentrations were measured using enzymatic reagent kits (Beckman Coulter, Fullerton, CA) according to the manufacturer's recommendations on the Synchron CX Delta System (Beckman Coulter).

Genotyping

DNA was extracted from tail tips using phenol-chloroform. For the crosses B6 × D2 and NZB × NZW, SNPs were genotyped by the Allele-Typing Service at The Jackson Laboratory in conjunction with KBiosciences (Hoddesdon, UK). For the crosses B6 × C3H and (NZO × NON) × NON, polymorphic MIT microsatellite markers were genotyped using agarose gel electrophoresis (NuSieve 3:1; FMC BioProducts, Rockland, ME). Markers were chosen at evenly spaced intervals where possible, and further details of the markers used are available in supplementary Tables I–IV. All data from these crosses are available in the Mouse Phenome Database in QTL archive under Su1 (jax.org/phenome; qtlarchive).

QTL analysis

QTL mapping was performed using R/QTL (version 1.07-12, available at http://www.rqtl.org) as described previously (32, 33). HDL, TC, and TG values were transformed using log base 10 to obtain a normal distribution (supplementary Fig. I). Main-effect QTL were computed at 2 centimorgan (cM) increments over the entire genome. QTL were deemed significant if they either met or exceeded the 95% genome-wide adjusted threshold,

TABLE 1. New and recent HDL and TG QTL mouse crosses

Cross	Sex	Diet	Marker[a]	HDL QTL[b]	TG QTL[b]	Ref.
(B6 × DBA/2J) F2	M	Chow	SNP	6	4	This report
(B6 × C3H/HeJ) F2	F	Ath	MIT	7	3	This report
(NZB × NZW) F2	F+M	Ath	SNP	10	4[c]	This report
(NZO × NON) × NON	M	Chow	MIT	2	2	This report
(B6 × 129) F2	F+M	Chow/Ath	SNP	19		(52)
(B6 × A/J) F2[d]	F+M	Chow	SNP	12	1	(55)
(NZB × RF) F2	F	Chow	MIT	3	1	(65)
(DUi6 × D2OlaHsd) F2	F+M	Chow	MIT	3		(66)
(B6.*Apoe*$^{-/-}$ × C3H.*Apoe*$^{-/-}$)F2	F	Chow	MIT	2		(67)
(DBA/1J × DBA/2J)[e]	F+M	Chow/Ath	SNP	5	18	(28)

[a] Complete marker lists for the crosses used in this study are provided in the supplementary tables. MIT, microsatellite marker.
[b] Number of QTL reported at time of publication.
[c] TG QTL have been reported in (32).
[d] In addition to the F2 cross, congenic strains were used with B6 backgrounds for Chrs 3, 8, and 11.
[e] Two-direction backcross.

which was assessed by 1,000 permutations; they were deemed suggestive if they either met or exceeded the 37% genome-wide adjusted threshold but were not significant (34). Approximate cM coordinates for markers were obtained by dividing base pair positions (mouse genome build 36) by a factor of 2 except for Chr 19, where Mb/1.04 was used. The validity of this approximation was confirmed by comparison to estimated map positions in R/QTL and also from previous cM-to-Mb comparisons in mouse (35). Simultaneous pair-wise genome scans were performed to detect gene interactions; however, no significant interactions were identified.

Combining crosses was performed as previously described (36). Briefly, genotypes from Chr 18 in the B6 × C3H and NZB × SM crosses were recoded, so that the B6 and SM genotypes became L for low HDL alleles and the C3H and NZB genotypes became H for high HDL alleles. A logarithm (base 10 of odds (LOD) score was computed at 2 cM intervals across the QTL interval for each cross separately and then for both crosses combined. The combined data were analyzed with "sex" and "cross" as additive covariates.

The raw data sets for each of these crosses, as well as multiple previously published HDL QTL studies, are available online in the Mouse Phenome Database (http://jax.org/phenome/qtlarchive).

SNP and haplotype analysis

Recently, >8 million SNPs were released for 16 mouse inbred strains (37). These data and several other sources were used to infer genotypes for a 50 strain set using a Hidden Markov Model; this imputed SNP resource is available at http://cgd.jax.org/ImputedSNPData/v1.1/ (38) and also in the Mouse Phenome Database on the center for genome dynamics (CGD) set of SNPs. SNPs for Chr 18 (n = 291,266) were downloaded, and locations that met the haplotype conditions were identified using a script implemented in the R statistical package. To carry out haplotype analysis, genomic regions within the QTL were excluded if the pair of strains that gave rise to a QTL had an identical haplotype pattern (B6 = C3H, B6 = DBA/2, and NZB = SM). Such regions are deemed identical by descent and are very unlikely to contain the causal genetic polymorphism underlying a common QTL (39). The remaining QTL regions were selected if the strains carrying the allele that increased HDL (C3H = D2 = NZB) were identical, if the strains carrying the allele that decreased HDL (B6 = SM) were identical, and if the haplotype pattern differed between the high and low allele strains (C3H, D2, NZB ≠ B6, SM). Gene lists for these regions were extracted from Ensembl (www.ensembl.org). These genes were examined in the Mouse Phenome Database (http://www.jax.org/phenome) for coding differences.

Sequencing

Additional sequencing was performed to confirm sequence variants between the different strains for *Mro* and *Lipg*. The genomic sequences of *Mro* (ENSMUST00000120033) and *Lipg* (ENSMUST00000066532) were obtained from the Ensembl (http://www.ensembl.org) mouse genome assembly, and primers were designed to amplify each exon, including at least 50 nucleotides of the adjacent introns. Sequences around noncoding SNPs were obtained from http://www.ncbi.nlm.nih.gov/SNP/. Standard PCR was performed using primers listed in supplementary Table V. Purified PCR products were subjected to thermocycle sequencing on capillary-based machines by the Jackson Laboratory DNA Sequence Laboratory. The sequence was analyzed using Sequencher software (version 4.1.4; GeneCodes Technology).

Chr 18/*Lipg* locus expression analysis

Liver mRNA expression levels were interrogated for the genes within the Chr 18 QTL region, narrowed after haplotype analysis to determine if parental strains for the three crosses (B6 × D2, B6 × C3H, and NZB × SM) differed in expression. The livers were obtained from five male and five female 12 week old mice of each strain fed chow or atherogenic diet. Total RNA was extracted from five mice of each strain-sex-diet group; three were chosen using random numbers from each group of five for microarrays, and all five were used for real-time PCR. Expression analysis was performed using Mouse Genome 430 2.0 Gene-Chip arrays (Affymetrix). The array data has been deposited at the Gene Expression Omnibus (www.ncbi.nlm.nih.gov/geo/; series number: GSE10493). RNA extraction, quantification, cDNA synthesis, and data analysis were carried out as described previously (40).

For real-time PCR, cDNA samples were mixed with SYBR Green Master Mix (Applied Biosystems, Foster City, CA) and gene-specific primers in a total volume of 25 μl. The primer pairs are as follows: *Lipg* forward 5′- TGGCTGCAGGAGAAGGAAGA-3′ and reverse 5′-CAGCGTGTAGGTATGCAGGA-3′ and β-*Actin* forward 5′-CTTCTTGGGTATGGAATCC-3′ and reverse 5′-GCTCAGGAGGAGCGGTGAT-3′. PCR was performed in 96-well optical reaction plates with an ABI PRISM 7500 sequence detection system (Applied Biosystems). Cycling parameters were 2 min at 50°C, 10 min at 95°C, and 40 cycles of 15 s at 95°C, and 1 min at 60°C. After PCR, a dissociation curve was constructed by increasing temperature from 65°C to 95°C for detection of PCR product specificity. PCR reactions were set up in triplicate for each strain-sex-diet group, and the expression of *Lipg* was normalized to the expression of β-actin.

Statistical analysis for complementation test

A least square means analysis was used to examine the interaction in F1 mice between *Lipg* (knockout or wild-type) by "allele" (high or low HDL in the crosses) for the quantitative complementation analysis. The null hypothesis for this test is that the difference in HDL between F1 mice carrying the wild-type alleles of *Lipg* and crossed to either the low HDL allele or high HDL allele strain at this QTL locus (Δ2) should not differ from the difference in HDL between F1 mice carrying $Lipg^{-/+}$ alleles (Δ1). If there was a significant difference ($P < 0.01$), then the candidate gene is considered to successfully complement. Data were analyzed using JMP version 7.0 (SAS Institute, Cary, NC).

RESULTS

HDL and TC QTL mapping

The four crosses (B6 × C3H, B6 × DBA/2, NZO × NON, and NZW × NZB) revealed 14 significant ($P < 0.05$) and 11 suggestive ($P < 0.63$) HDL QTL on Chrs 1–6, 8, 11, 12, 15, 16, 18, and 19 (**Fig. 1**; **Table 2**). All HDL QTL have been identified in other mouse crosses (27), except those on Chrs 1, 8, 12, and 16 observed in the NZB × NZW cross. Distal Chr 1 was the most frequently identified QTL, observed in three crosses, including B6 × D2, B6 × C3H, and (NZO × NON) × NON, and its causal gene is most likely *Apoa2* (41). A second locus with a peak at 49 cM on Chr 1 was identified in the cross NZB × NZW. Recently, *Farp2* and/or *Stk25* were reported as the candidate genes for this QTL using the NZB × NZW cross (42); both genes have some evidence, but further evidence is needed to choose between the two. Three significant QTL were identified

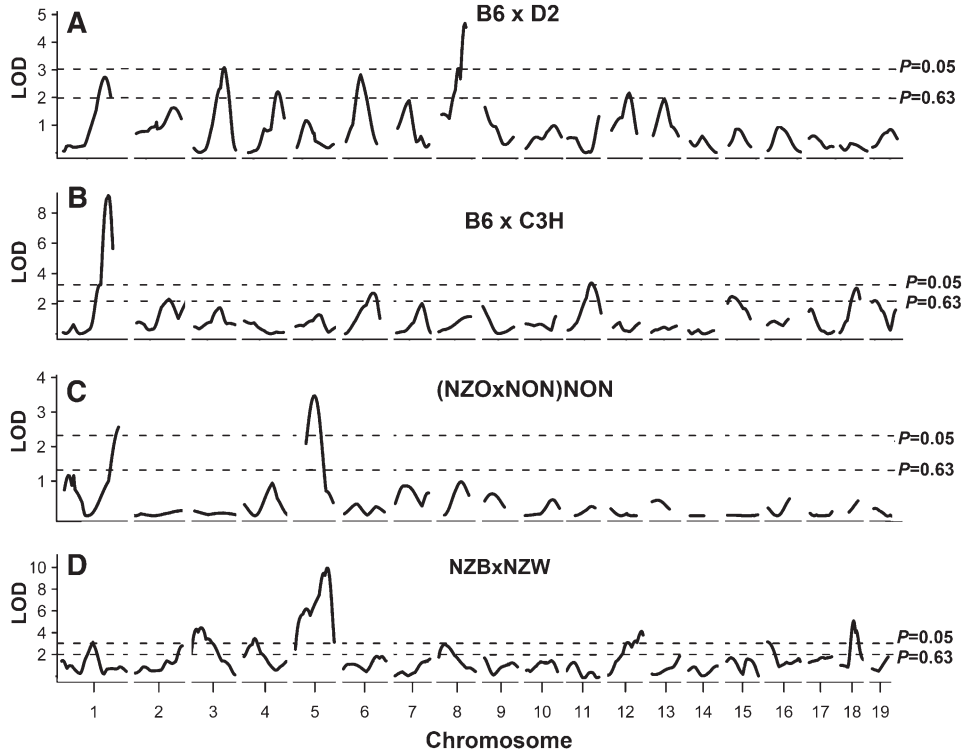

Fig. 1. Genome-wide scans for HDL. A: B6 × D2. B: B6 × C3H. C: (NZO × NON) × NZO. D: NZB × NZW. The horizontal dashed lines represent suggestive ($P = 0.63$) and significant ($P = 0.05$) levels as determined by 1,000 permutation tests.

on Chr 5 at 26 cM (LOD = 9.0) and 57 cM (LOD = 12.7) in the NZB × NZW cross and at 41 cM (LOD = 3.4) in the (NZO × NON) × NON cross. Interestingly, HDL levels are raised by heterozygous alleles for the Chr 5 QTL in the (NZO × NON) × NON cross. It has been previously shown that heterotic effects in an NZO × NON outcross exacerbated both diabesity and perturbations in lipid metabolism (43). Two significant QTL were identified on Chr 3 at 26 cM (LOD = 4.5, NZB × NZW cross) and at 64 cM (LOD = 3.0, B6 × D2 cross). All these QTL have been observed multiple times in other crosses (27).

For TC, in the chow-fed crosses B6 × D2 and (NZO × NON) × NON, three suggestive QTL distributed on Chrs 2, 7, and 8 were identified specifically for TC; the other seven QTL were identified for both TC and HDL. This indicates that the majority of the cholesterol QTL observed in mice maintained on a chow diet are represented by HDL loci. In the atherogenic diet-fed crosses, B6 × C3H and NZB × NZW, 11 QTL were identified for TC, six of them (54.5%) were independent of HDL QTL (Table 2; see supplementary Fig. II). This indicates that nonHDL cholesterol levels differ between strains after consuming atherogenic diet and yield QTL different from HDL loci.

TG QTL mapping

Five significant TG QTL were identified (**Fig. 2**; Table 2). Two were mapped at approximately the same location on Chr 2 at 73 cM (LOD = 2.4) in (NZO × NON) × NON and 80 cM (LOD = 4.7) in B6 × C3H, and these shared approximately the same confidence interval. Three additional significant QTL were mapped located on Chr 12 in the B6 × D2 cross (14 cM, LOD = 3.1), Chr 18 in the B6 × C3H cross (39 cM, LOD = 3.2), and distal Chr 1 near the HDL/*Apoa2* locus (89 cM, LOD = 3.5) in the (NZO × NON) × NON cross. Previously reported QTL for the NZB × NZW cross mapped to Chr 7 (50 cM, LOD = 3.1) and Chr 8 (11 cM, LOD = 3.2) (32).

TG levels were positively correlated with HDL levels in three crosses; however, for all three crosses, the proportion of TG explained by the relationship of TG to HDL was small; B6 × C3H ($r^2 = 0.14$, $P < 0.0001$), B6 × D2 ($r^2 = 0.05$, $P < 0.0001$), and NZB × NZW ($\mathbf{r}^2 = 0.03$, $P = 0.0068$). TG levels were not correlated with HDL in the (NZO × NON) × NON cross. A stronger correlation between TG and HDL was not predictive of more overlapping HDL and TG QTL. Nonetheless, five significant TG QTL (Chrs 1, 2, 8, 12, and 18) had overlapping 95% confidence intervals with HDL QTL (Table 2).

Combining crosses and haplotype analysis reduced the Chr 18 HDL QTL to six genes

Several crosses detected HDL QTLs on Chr 18 as listed in **Table 3**. The LOD score plots for the crosses, where available, are reproduced in **Fig. 3A**. These LOD score plots indicate as many as four Chr 18 QTL at 23, 55, 77, and 85 Mb. Table 3 lists which crosses contain each QTL (if the LOD score plots are not available, the reported peak and confidence intervals were used to estimate the presence or absence of the QTL with surrounding regions denoted by "–?"). Further analysis presented here focuses

TABLE 2. Significant and suggestive lipid QTL from four new mouse crosses

	HDL				TC				TGs			
Chr	QTL[a]	Peak cM[b] (95% CI)	LOD[c]	High Allele (Effect)[d]	QTL[a,e]	Peak cM[b] (95% CI)	LOD[c]	High Allele (Effect)[d]	QTL[a]	Peak cM[b] (95% CI)	LOD[c]	High Allele (Effect)[d]
B6 × D2												
1	*Hdlq15*	85 (69–94)	2.8	D2 (dom)	*Hdlq15*	83 (73–93)	3.1	D2 (dom)				
2						76 (10–84)	2.2	D2 (add)				
3	*Hdlq21*	64 (50–70)	**3.0**	B6 (dom)	*Hdlq21*	66 (42–72)	2.1	B6 (dom)				
4	*Hdlq64*	63 (38–75)	2.2	D2 (dom)								
6	*Hdlq11*	37 (23–51)	2.8	D2 (add)	*Hdlq11*	38 (23–55)	2.3	D2 (add)				
7						28 (8–40)	2.4	B6 (add)		22 (8–56)	2.3	B6 (dom)
8	*Hdlq16*	56 (42–56)	**4.6**	B6 (add)	*Hdlq16*	56 (50–56)	**4.6**	B6 (add)				
10										49 (29–80)	2.3	B6 (add)
12	*Hdlq63*	42 (14–52)	2.2	B6 (add)	*Hdlq63*	36 (8–48)	2.6	B6 (add)	*Tgq33*	14 (5–28)	**3.1**	B6 (add)
16										5 (3–19)	2.1	D2 (dom)
B6 × C3H												
1	*Hdlq15*	86 (84–90)	**9.1**	C3H (add)	*Tcq3*	84 (42–92)	2.4	C3H(add)				
2		60 (44–87)	2.4	C3H (add)					*Tgq32*	80 (64–87)	**4.7**	C3H (add)
3						72 (15–77)	2.6	B6 (dom)		58 (37–65)	2.5	C3H (add)
6		60 (36–70)	2.7	B6 (add)								
11	*Hdlq74*	42 (35–54)	**3.2**	C3H(add)								
15		26 (4–38)	2.5	B6 (dom)								
17						4 (2–30)	2.4	C3H(dom)				
18	*Hdlq76*	37 (32–42)	2.8	C3H(rec)					*Tgq34*	39 (19–42)	**3.2**	C3H (add)
19	*Hdlq48*	4 (3–30)	2.1	B6 (dom)								
(NZO × NON) × NON												
1	*Hdlq69*	92 (5–92)[f]	**2.4**	NON	*Hdlq69*	92 (75–92)	**3.5**	NON	*Tgq30*	89 (73–92)	**3.5**	NON
2									*Tgq31*	73 (66–80)	**2.4**	NON
5	*Hdlq73*	41 (27–49)	**3.4**	Het[g]	*Hdlq73*	43 (31–53)	**3.8**	Het[g]				
8					*Tcq7*	36 (24–54)	1.5	Het[g]				
NZB × NZW[h]												
1	*Hdlq68*	49 (40–63)	**3.3**	NZW(rec)		49 (30–62)	2.7	NZW(rec)				
2	*Hdlq70*	82 (70–84)	2.8	NZB(dom)	*Tcq4*	83 (48–83)	**4.0**	NZB(dom)				
3	*Hdlq71*	26 (15–37)	**4.5**	NZB(rec)								
4	*Hdlq72*	25 (13–34)	**3.5**	NZW(add)						22 (11–33)	2.1	NZW(rec)
5	*Hdlq7*	26 (15–36)	**9.0**	NZB(add)								
5	*Hdlq8*	57 (52–62)	**12.7**	NZB(add)	*Tcq5*	61 (51–65)	**7.9**	NZB(add)				
7					*Tcq6*	62 (35–62)	2.9	NZW(rec)	*Tgq4*	50 (29–58)	**3.1**	NZW(add)
8		18 (11–33)	2.9	NZB(add)					*Tgq5*	11 (0–25)	**3.2**	NZW(add)
9					*Tcq8*	53 (50–58)	**7.7**	NZB(add)				
11						12 (9–27)	2.4	NZB(dom)				
12	*Hdlq75*	54 (41–56)	**4.1**	NZB(add)								
14						25 (6–42)	2.4	NZB(dom)				
16	*Hdlq76*	2 (2–17)	**3.2**	NZW(cd)								
18	*Hdlq77*	30 (28–32)	**5.1**	NZB(cd)	*Tcq9*	33 (29–36)	**5.8**	NZB(rec)	*Tgq6*	34 (26–39)	**4.1**	NZB(rec)

[a] QTL were named if they were significant or if they were suggestive but confirmed QTL reported previously. They were given the same name if the crosses identifying them shared at least one common parental strain and a new name if the crosses identifying them involved no common strains.

[b] cM is Mb converted by factor of 2 validated by Moran et al. (35). CI, confidence interval.

[c] The significant LOD scores determined by 1,000 permutation tests are given in bold.

[d] Dom, dominant; add, additive; rec, recessive; cd, codominant.

[e] In chow-fed crosses B6 × D2 and (NZO × NON) × NON), same names were assigned if HDL QTL colocalized with TC QTL; in atherogenic diet-fed crosses (B6 × C3H and NZB × NZW), different names were assigned even if colocalized with HDL QTL.

[f] Second suggestive peak at around 10 cM.

[g] In backcross, a high allele in the heterozygous state is probably due to an additive or dominant effect of the minor allele in NZO.

[h] TG QTL from this cross have been reported in (32).

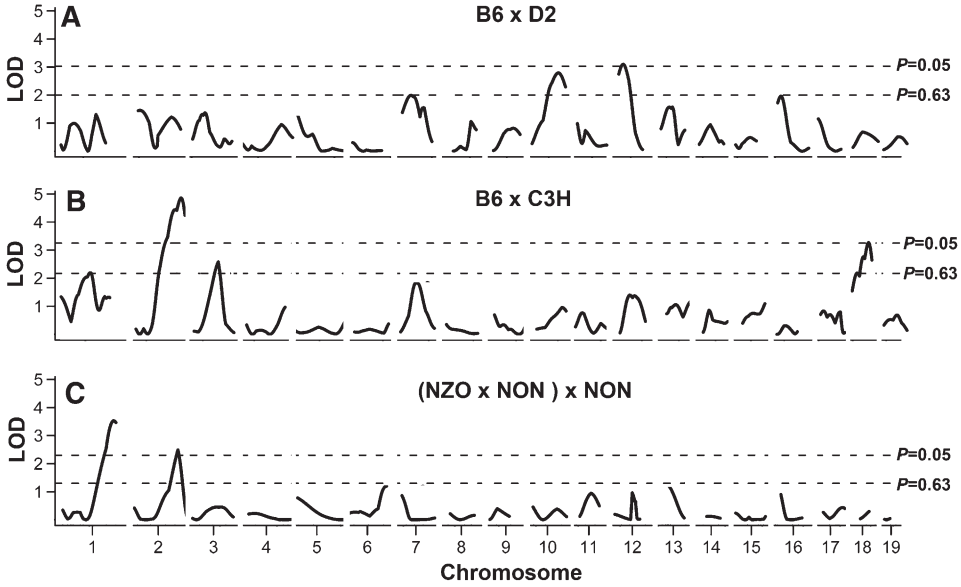

Fig. 2. Genome-wide scans for TG. A: B6 × D2. B: B6 × C3H. C: (NZO × NON) × NZO. The horizontal dashed lines represent suggestive ($P = 0.63$) and significant ($P = 0.05$) levels as determined by 1,000 permutation tests.

on the Chr 18 QTL at 77 Mb, which is found in at least four crosses: B6 × C3H, B6 × D2, NZB × SM, and B6 × CAST. The allele causing high HDL in these crosses was C3H, D2, NZB, or CAST. From the LOD score curves, it can be seen that the B6 × 129 and the NZB × NZW crosses detect a QTL at 55 Mb but not at 77 Mb (Fig. 3A).

The B6 × D2 cross reported in this article did not detect the Chr 18 QTL, but another B6 × D2 cross in the literature carried out in female mice did detect a Chr 18 QTL (44). It is not clear why the B6 × D2 cross reported here failed to detect a Chr 18 QTL; however, the complementation test discussed below shows some consistency with this observation. The mode of inheritance differs for some of these crosses, but the mode of inheritance may be influenced or obscured by a closely linked QTL, especially if it is stronger, or by the genetic background. Thus, the different modes of inheritance should not hinder combined cross analysis (36, 45).

Combining crosses can be a powerful method for narrowing QTL. If the QTL in separate crosses are caused by the same gene, then combining crosses will increase the LOD score and narrow the confidence interval; if the hypothesis that the QTL are caused by the same gene is incorrect, the LOD score will not increase and the confidence interval remains the same or increases. Combining crosses requires access to the raw data, and for the Chr 18 QTL at 77 Mb, data are available only for the crosses B6 × C3H and NZB × SM. To combine the data, the genotype information was recoded from a strain-specific code to a phenotype-specific code; B6 and SM genotypes became L for the low HDL allele, while C3H and NZB genotypes became H for the high HDL allele. This analysis reduced the QTL to a 9 Mb region spanning from 72–81 Mb (Figs. 3B and **4A**). The QTL was further narrowed by reducing the region to that overlapping the human QTL at 18q12.1-22.2 (46), thus reducing the region to 6.9 Mb and 42 genes (Fig. 4A, step c).

The QTL was further narrowed by haplotype analysis using the same two crosses as well as adding the B6 × D2 cross (44). The B6 × CAST cross could also be included;

TABLE 3. Crosses that detected a QTL on Chr 18

Cross	Diet	Sex	High Allele	Peak (Mb)	95% CI	Common Peak Chr 18 QTL Location[a]				Ref.
						23 Mb	55 Mb	77 Mb	85 Mb	
B6 × C3H	Chow, ath	F	C3H	66	31–73	–	X	X	–	(68)
B6 × C3H	Ath	F	C3H	74	64–84	–	X	X	X	–[b]
B6 × D2	Chow	F	D2	73	60–86	–?	–?	X	–?	(44)
B6 × CAST	Ath	F, M	CAST	76	62–87	–?	–?	X	–?	(69)
NZB × SM	Chow, ath	F, M	NZB	84	69–91	X[c]	X	X	X	(70)
NZB × NZW	Ath	F, M	NZB	60	54–64	–	X	–	–	–[b]
B6 × 129	Chow	F, M	129	23	10–36	X	–	–	–	(52)
B6 × 129	Chow	F, M	129	52	36–63	–	X	–	–	(52)

[a] No QTL detected indicated by "–," while an X indicates the presence of a QTL with an interval spanning a common peak location found in other crosses. For some published QTL, data were lacking to determine the exact confidence interval of the QTL; therefore, the surrounding regions are by denoted by "–?".

[b] QTL are reported for the first time in this article.

[c] The QTL was found in chow-fed animals only.

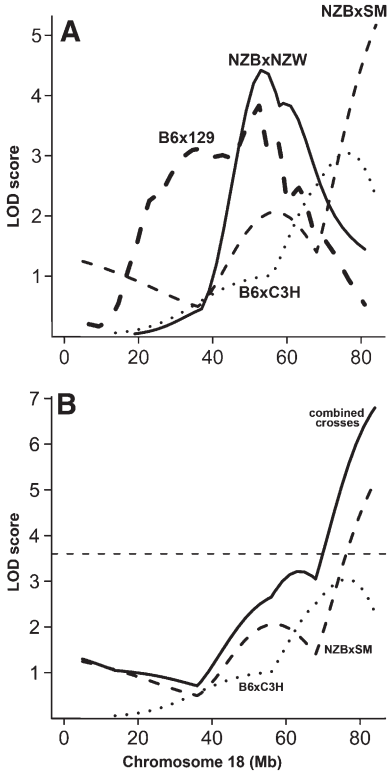

Fig. 3. LOD score plots for the QTLs on distal chromosome 18. A: The LOD score plots are shown for B6 × C3H (dotted line), NZB × SM (thin dashed line), NZB × NZW (solid line), and B6 × 129 (thick dashed line). Raw data for B6 × D2 (44), B6 × CAST (69), and B6 × C3H (68) listed in Table 3 are not available for reproduction. B: The LOD score plot obtained by combining the B6 × C3H and the NZB × SM crosses is shown as a solid line. The horizontal dashed line represents the significance threshold level ($P = 0.05$) as determined by 1,000 permutation tests.

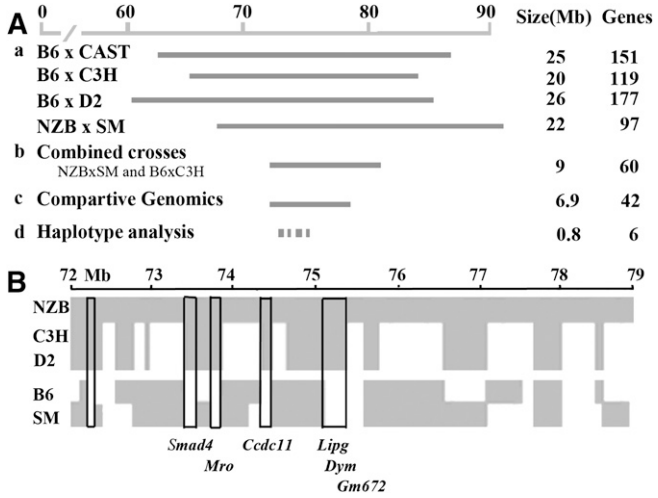

Fig. 4. HDL QTL on chromosome 18 narrowed to six genes by haplotype analysis. A: The 95% confidential intervals for each individual cross with a peak at 77 Mb (a) and the combined cross interval (b). Comparative genomics comparing human HDL QTL that overlap this region further narrows the target region (c). Haplotype analysis reduces the interval to small regions containing six genes (d). B: An enlargement of the haplotype analysis; regions highlighted in blocks show the locations where the high allele strains (NZB, C3H, and D2) are identical by descent, where the low allele strains (B6 and SM) are identical by descent, and where the high strains differ from the low strains.

however, strains recently derived from the wild such as CAST may not share the identical by descent regions of the classic inbred strains so haplotyping is often uninformative, as in this case (data not shown). Haplotyping is based on the assumptions that the gene causing the QTL is the same in all three crosses and that the mutation is an ancestral mutation, which is reasonable since it was found in multiple crosses. Of the approximately 300,000 SNPs available for Chr 18, approximately 30,000 mapped within the QTL confidence interval. These SNPs were interrogated to identify regions that fit the following criteria: the strains that carry the allele that increased HDL had identical haplotypes (C3H, D2, and NZB), the strains that carry the allele that decreased HDL had identical haplotypes (B6 and SM), and these two haplotypes differed from each other. This haplotype analysis reduced the QTL region to six genes as potential candidates: *Smad4*, *Mro*, *Ccdc11*, *Lipg*, *Dym*, and *Gm672* (Fig. 4).

Further analysis of the six genes by sequence and expression differences

It is expected that the QTL gene should have a difference in function caused by an amino acid change in the coding region or a noncoding sequence difference that alters expression levels, mRNA stability, splice sites, or other regulatory regions. Analysis of the coding SNPs in these six genes (Mouse Phenome Database; www.jax.org/phenome/SNP) revealed two genes with SNPs that caused nonsynonymous amino acid changes: Asp218Glu in maestro (*Mro*) and Tyr262Cys in endothelial lipase (*Lipg*). These two SNPs were resequenced in B6, C3H, and D2 to confirm the public data and also in NZB and SM, strains that had not previously been genotyped for these SNPs. However, sequencing showed that strains NZB and SM did not differ at the SNP in *Mro*, making *Mro* an unlikely candidate gene. Following resequencing of *Lipg*, the reported SNP in D2 causing the Tyr262Cys change, originally identified by Mural et al. (47), was shown to be an error; all five strains have Tyr-262. Sequencing *Mro* and *Lipg* exons for all five strains showed that except for the Asp218Glu *Mro* SNP (B6 = Asp; C3H, D2, NZB, and SM = Glu), there was no other coding variants among these strains for *Mro* and *Lipg* coding regions. Consequently, a coding region sequence variant causing a functional change is not likely to be the cause of this common QTL.

Since these six genes do not appear to have a coding region polymorphism that alters protein function, the QTL may be mediated by a sequence variant affecting differences in the mRNA. To further characterize the Chr 18 QTL, microarrays were used to examine gene expression of the six genes (**Table 4**). Parental expression of these genes from mouse livers from each parental strain-sex-diet group (n = 3) giving rise to the original QTL were examined. The three original Chr 18 QTL yield six strain-sex-diet comparisons: NZB × SM (males and females on chow and high-fat atherogenic diet), D2 × B6 (females on chow), and C3H × B6 (females on high-fat atherogenic diet). Of

TABLE 4. Liver expression comparisons for probe sets representing genes narrowed by haplotype analysis

		D2 Relative B6		NZB Relative to SM								C3H Relative B6	
	Sex, Diet	F, Chow		F, Chow		F, HF-Ath		M, Chow		M, HF-Ath		M, HF-Ath	
Probe ID	Gene	FC	FDR	FC	FDR	FC	FDR	FC	FDR	FC	FDR	FC	FDR
1422485_at	*Smad4*	**-1.9**	**0.002**	1.0	n.s.	1.0	n.s.	1.0	n.s.	1.0	n.s.	**-2.1**	**0.000**
1430588_at	*Mro*	−1.0	n.s.	1.0	n.s.	−1.1	n.s.	1.1	n.s.	1.0	n.s.	−1.0	n.s.
1453868_at	*Ccdc11*	−1.1	n.s.	1.0	n.s.	1.0	n.s.	1.0	n.s.	−1.1	n.s.	−1.1	n.s.
1421262_at	*Lipg*	**-1.5**	**0.029**	**-2.0**	**0.004**	**-1.7**	**0.001**	**-1.7**	**0.001**	**-1.4**	**0.005**	−1.0	n.s.
1430532_at	*Dym*	−1.1	n.s.	−1.1	n.s.	1.0	n.s.	−1.1	n.s.	1.0	n.s.	−1.0	n.s.
1427743_at	*Gm672*	−1.2	n.s.	−1.3	n.s.	**-1.7**	**0.000**	1.0	n.s.	**-1.5**	**0.006**	−1.2	n.s.

The array data have been deposited at http://www.ncbi.nlm.nih.gov/geo/ (series: GSE10493). Each sex-diet-strain is composed of n = 3 mice, giving rise to a total of 18 mice surveyed with the low-allele compared with high-allele strains. Comparisons with a false discovery rate (FDR) < 0.05 are indicated in bold. The allele for high HDL is listed first in each comparison. FC, fold change; n.s. not significant; F, female; M, male.

the six genes identified through haplotyping, only *Lipg* is consistently significantly differentially expressed (five of six possible comparisons, false discovery rate < 0.05). Two other probe sets have two of six possible comparisons that are significant (Table 4). *Lipg* expression was confirmed by real-time PCR in mouse livers (n = 5/strain-sex-diet group) among all the parental strain combinations that detected the Chr 18 QTL. In this case, *Lipg* expression was observed to be significantly different in all six comparisons with lower expression in the NZB, D2, and C3H strains carrying the allele that increased HDL compared with the B6 and SM strains carrying the allele that decreased HDL levels (**Fig. 5**). Thus, *Lipg* is the most likely candidate gene, and there must be a sequence polymorphism that affects its expression.

To find the polymorphism that regulates *Lipg* expression, transcription factor binding sites in the upstream region of *Lipg* were examined using public SNPs with TRANSFAC software (http://www.biobase.de/pages/index.php?id = 271). Two SNPs between the low-allele strain B6 and high-allele strains C3H and D2 are inside or right next to putative transcription factor binding sites for c-ETS-1 and v-MYB (**Table 5**), and an additional 10 SNPs

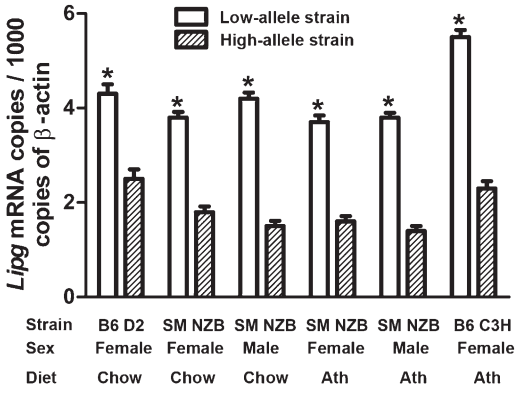

Fig. 5. *Lipg* mRNA analysis in parental strains involved in the HDL QTL crosses. Real-time gene expression to confirm microarray observations; total RNA was extracted from mouse livers (n = 5 per sex-strain-diet group leading to a total of n = 30 for low-allele mice and n = 30 high-allele mice for a total of 60 independent mice). Expression levels of *Lipg* are normalized to β-actin and expressed as mRNA copies per 1,000 copies of β-actin. *$P < 0.01$ compared with the expression in high allele strain.

are near transcription factor binding sites. These SNPs were also sequenced for NZB and SM if the public databases were missing data for these strains. These SNPs are arranged in genomic order for all the strains that were parents of QTL crosses that detected a QTL on Chr 18, including the two crosses B6 × 129 and NZB × NZW that do not detect the QTL at 77Mb, but rather detecting an independent QTL at the 55 Mb locus (Table 5). Strains B6, SM, and 129 share the same haplotype block, while strains NZB, NZW, C3H, and D2 fall into a second haplotype block (gray region of Table 5). This shows that B6 × 129 and NZW × NZB crosses could not have detected the QTL caused by *Lipg* because the parental strains are identical to each other. CAST has its own unique haplotype typical of a wild-derived strain (data not shown).

Deficiency complementation of *Lipg*

Lipg has a known role in HDL metabolism, and its knockout and transgene alter HDL levels. However, as a further test of its role as the causal gene for this QTL, we carried out a deficiency complementation test (48, 49). In such a test, the B6.129-*Lipg*$^{-/-}$ strain is mated to both parents of a QTL cross. As a control, the B6 strain is mated to the same parents. The four different F1 populations are tested for HDL levels. The null hypothesis for a deficiency complementation test is that the difference (Δ2 in **Fig. 6**) between F1 mice that carry the *Lipg* wild-type gene is the same as the difference (Δ1 in Fig. 6) between F1 mice that are heterozygous for the *Lipg* knockout. If Δ1 is equal to Δ2, then reduced expression of *Lipg* in the *Lipg*$^{-/+}$ F1 has no effect on HDL and there is no complementation between *Lipg* expression levels and the high or low HDL allele. However, if Δ1 differs significantly from Δ2, then the *Lipg* allele from the knockout complements the *Lipg* allele in one parental strain, indicating that the knockout gene and the QTL gene are the same. We crossed B6.129-*Lipg*$^{-/-}$ and strain B6 (B6.*Lipg*$^{+/+}$) to each of the parents of the three crosses that detected the QTL, to strains B6 and C3H (Fig. 6A), to strains B6 and D2 (Fig. 6B), and to strains NZB and SM (Fig. 6C). As shown in Fig. 6, in each case, Δ2 was significantly larger than Δ1 ($P < 0.001$), indicating that *Lipg* did complement and is therefore the QTL gene. For the B6 × D2 complementation test (Fig. 6B), the change between Δ2 and Δ1 in females is considerably greater than it is between males, which may explain why this QTL was

TABLE 5. Analysis of SNPs in or near transcription factor binding sites upstream of *Lipg*

Binding Site				SNPs Upstream of *Lipg*								
						Strains[c]						
TF[a]	Start bp	End bp	Bases[b]	ID	bp	B6	SM	129	C3H	D2	NZB	NZW
TCF11	-8,850	-8,838	**G**TCATgttatcct	rs36403956	-8,850	G	G		T	T	G	
RFX	-10,053	-10,045	cgGCAACtg	rs38555666	-10,065	C	C	C	T	T	T	T
PAC1	-12,250	-12,237	tcattGTTTTgttt	rs38319702	-12,256	T	T	T	A	A	A	A
HSF1	-16,765	-16,756	AGAAGgttct	rs38760079	-16,774	C	C	C	T	T	T	T
Hand1:E47	-16,938	-16,923	gattCCAGAcaataga	rs36754426	-16,940	G	G	G	A	A	A	A
c-ETS-1	-17,288	-17,276	atac**CG**GAAatcc	rs38875977	-17,283	G	G	G	A	A	A	A
PAX-5	-19,824	-19,807	gggagctcagAGGCGgga	rs30824477	-19,860	G	G	G	T	T	T	T
GFI1	-21,421	-21,409	agaAATCAatggt	rs38079734	-21,407	C	C	C	T	T	T	T
GFI1	-21,421	-21,409	agaAATCAatggt	rs39235685	-21,431	A	A	A	G	G	G	G
v-MYB	-21,718	-21,710	tCCGTT**g**a**c**	rs38231440	-21,711	A	A	A	G	G	G	G
NKX2-5	-23,177	-23,168	gaAAGTGaaa	rs36956394	-23,181	A	A	A	G	G	G	G
KID3	-23,401	-23,397	CCACG	rs37165546	-23,405	A	A	A	G	G	G	G

The first SNP rs36403956 does not match the required haplotype since NZB and SM are identical, indicating the upper boundary of the haplotype block. Underlined SNPs indicate that the polymorphism is located in the transcription factor binding site.

[a] Location is relative to the *Lipg* 5′ untranslated region on mouse Chr 18.

[b] Uppercase indicates the TF binding site, and lowercase represents flanking bases necessary for TF binding. Bold underlined bases indicate the SNPs located in the binding sites or conserved neighboring base pairs required for efficient binding.

[c] SNPs for SM and NZB were sequenced, while SNPs for B6, C3H, D2, 129, and NZW are publically available at the Mouse Phenome Database (http://phenome.jax.org/pub-cgi/phenome/mpdcgi?rtn = snps/door). Region in gray shows haplotype block that likely contains the regulatory element controlling the *Lipg* QTL. TF, transcription factor.

detected in a female cross and not in the male cross reported here.

The complementation test works best when both the QTL and the knockout are fully recessive (50). However, heterozygous *Lipg*$^{-/+}$ mice are additive for the HDL phenotype (51). Although in the B6 × C3H QTL, the C3H allele is recessive, the QTL shows additive inheritance in the B6 × D2 and the NZB × SM cross. It is interesting that the complementation test worked just as well for these crosses, showing additive inheritance as for the cross showing the recessive inheritance. This indicates that while it is not optimal to have both the knockout gene and the QTL gene show additive inheritance, it does not rule out the possibility of observing complementation as we did for all three crosses.

It is also important to note that the *Lipg*$^{-/-}$ mice are not on a pure B6 background. This raises the possibility that passenger genes from the 129 strain could have caused the results we observe in the complementation test. However, this is unlikely because no QTL for HDL levels is present in the *Lipg* region, as demonstrated recently in a large (n = 528) F2 cross between B6 and 129/S (52) and by the haplotype pattern in Table 5 showing that B6 and 129 are identical in the *Lipg* region.

DISCUSSION

To identify QTL genes, traditional techniques have relied upon genetic methods such as further mapping through the creation of congenic strains (53, 54). However, with the availability of dense SNPs for most of the common inbred strains (37, 38), fine mapping QTL should be easier since many of the polymorphic regions in any cross will be known. Furthermore, the ability to combine crosses based on the assumption that the causal alleles are ancestral demonstrates a need for further QTL studies. Generating an F2 or backcross population may be more efficient than constructing a set of congenic strains and can help map multiple common QTL (55).

In this study, four additional mouse crosses are reported for HDL, bringing the total number of HDL QTL studies to 35. HDL is one of the most characterized quantitative phenotypes in mouse models, second only to obesity and body weight phenotypes (56). However, as most crosses were originally performed with varying purposes, focusing on specific diets or sexes or optimizing the study for atherosclerosis phenotypes (57), identifying causal genes through haplotyping and combined crosses remains a challenge. The four crosses described here identify HDL

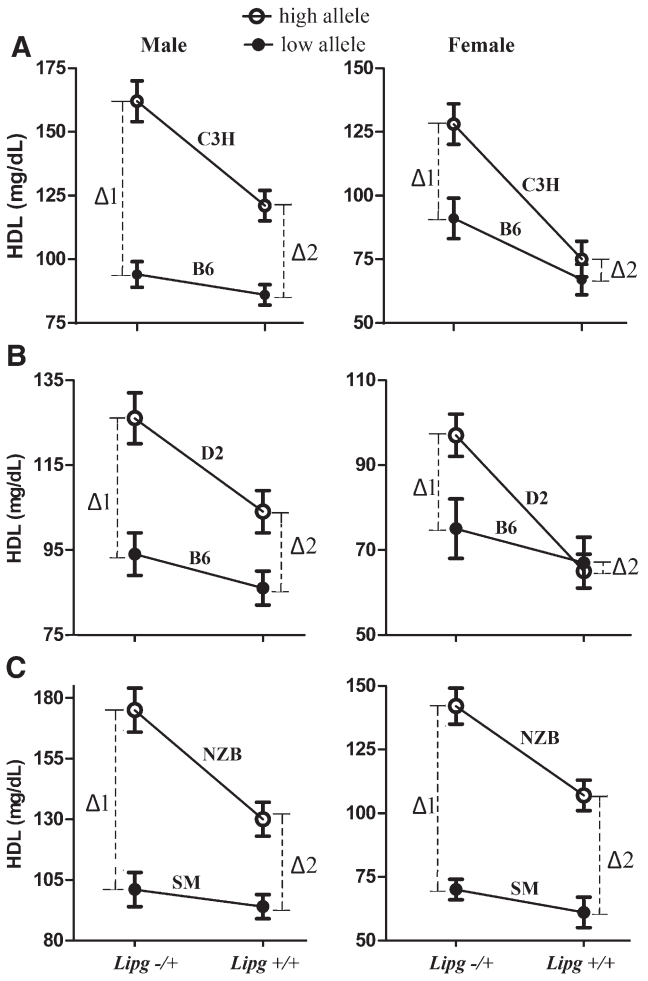

Fig. 6. Complementation test of parental strains with *Lipg*$^{-/-}$. Data for HDL presented as means (mg/dl) ± SD. The number of F1 mice used for each group is n = 10–15. Open circles are the high allele strains (C3H, D2, and NZB); closed circles are the low allele strains (B6 and SM). A: B6 × C3H cross. B: B6 × D2 cross. C: NZB × SM cross. The deficiency complementation consists of comparing Δ1 with Δ2; if there is no complementation, Δ1 = Δ2 and lines are parallel. If there is complementation, the two deltas are significantly different from each other and the lines are not parallel. *P* values were calculated using two-way ANOVA test in JMP software. For all comparisons, $P < 0.001$.

QTL, most of which have been replicated in previous studies, indicating that the QTL are controlled by ancestral mutations common among inbred strains.

The additional crosses allow for one more HDL QTL gene, *Lipg*, to be identified. For the Chr 18 QTL, combining crosses and haplotype analysis based primarily on the dense resequencing of B6, D2, and C3H (http://mouse.perlegen.com/mouse/) identified six likely candidates. Sequence analysis revealed that these genes did not contain coding sequence variants that could explain the QTL. However, an examination of expression analysis reveals that of the six genes narrowed by haplotype, only *Lipg* is consistently differentially expressed between relevant strains. Indeed, when examining all 165 probe sets in the 95% combined-cross confidence interval (data not shown), *Lipg* remains the most consistently differentially regulated gene with five of six possible significant differences by microarray analysis (Table 4). Furthermore, for *Lipg*, there is a consistent pattern whereby the strains with the high HDL allele expressed lower *Lipg* mRNA compared with the strains with the low HDL allele (Fig. 5). Finally, a deficiency complementation test implicates *Lipg* as the gene involved in three of the QTL on distal Chr 18. In this test, the interaction of *Lipg* genotype with either high- or low-allele strains was significant, demonstrating complementation of *Lipg* with the Chr 18 HDL QTL. Likely it is this consistent difference in expression levels, caused by a noncoding polymorphism that causes the distal Chr 18 HDL QTL. The relevant haplotype region contains at least two transcription factor binding sites with such a polymorphism.

The results presented here for *Lipg* are consistent with the gene function and the phenotypes observed both in *Lipg* knockout mice and transgenic mice. *Lipg* encodes endothelial lipase, and endothelial lipase hydrolyzes HDL phospholipids in vivo, thus generating smaller phospholipid-depleted HDL particles that are more rapidly catabolized by both the kidney and the liver (58). *Lipg* knockout mice have increased HDL levels along with increased plasma cholesterol, phospholipids, and associated apolipoproteins (51, 59). Overexpression of human *Lipg* in mice results in a significant decrease in HDL cholesterol and apolipoprotein A-I levels (59).

In humans, *Lipg* maps to 18q21.32 and is included in a human QTL for HDL (46) and apolipoprotein A-I levels (60). It has been shown that apolipoprotein A-I is involved in the pathway modulating endothelial lipase function and HDL regulation (61). In addition, associations between LIPG SNPs or haplotypes and HDL have been found in several human studies (51, 62, 63) with indications that SNPs in regulatory regions are important (64). Exactly which and how distant the regulatory regions operate to regulate *Lipg* remains an important question that further mouse studies could help address in the future.

The number of QTL crosses available for meta-analysis is a limiting factor; however, as more data sets become available, the ability to fine map the causal genes should also increase. This strategy relies heavily on the quality of databases, in particular the accuracy of SNPs. Currently, it is estimated that there is a ~57% false-negative rate of discovery in the mouse inbred strain data set (37). Even a single SNP between two strains is sufficient for a QTL, and this can be overlooked by such an approach, requiring a broader application of tools such as complementation testing to prove candidate genes. However, as SNP databases increase in both size and accuracy, the false-negative rate should decline, and the success rate of identifying QTL genes should improve.

The authors thank Dr. Keith DiPetrillo who performed the B6 × D2 cross, Peter Reifsnyder and Pam Stanley who performed the (NZO × NON) × NON cross, and Harry Whitmore and Susan Sheehan for excellent technical assistance.

REFERENCES

1. Sarwar, N., J. Danesh, G. Eiriksdottir, G. Sigurdsson, N. Wareham, S. Bingham, S. M. Boekholdt, K. T. Khaw, and V. Gudnason. 2007. Triglycerides and the risk of coronary heart disease: 10,158 incident cases among 262,525 participants in 29 Western prospective studies. *Circulation.* **115:** 450–458.
2. Singh, I. M., M. H. Shishehbor, and B. J. Ansell. 2007. High-density lipoprotein as a therapeutic target: a systematic review. *JAMA.* **298:** 786–798.
3. 1975. Clofibrate and niacin in coronary heart disease. *JAMA.* **231:** 360–381.
4. 2000. Secondary prevention by raising HDL cholesterol and reducing triglycerides in patients with coronary artery disease: the Bezafibrate Infarction Prevention (BIP) study. *Circulation.* **102:** 21–27.
5. Brown, B. G., X. Q. Zhao, A. Chait, L. D. Fisher, M. C. Cheung, J. S. Morse, A. A. Dowdy, E. K. Marino, E. L. Bolson, P. Alaupovic, et al. 2001. Simvastatin and niacin, antioxidant vitamins, or the combination for the prevention of coronary disease. *N. Engl. J. Med.* **345:** 1583–1592.
6. Canner, P. L., K. G. Berge, N. K. Wenger, J. Stamler, L. Friedman, R. J. Prineas, and W. Friedewald. 1986. Fifteen year mortality in Coronary Drug Project patients: long-term benefit with niacin. *J. Am. Coll. Cardiol.* **8:** 1245–1255.
7. Frick, M. H., O. Elo, K. Haapa, O. P. Heinonen, P. Heinsalmi, P. Helo, J. K. Huttunen, P. Kaitaniemi, P. Koskinen, V. Manninen, et al. 1987. Helsinki Heart Study: primary-prevention trial with gemfibrozil in middle-aged men with dyslipidemia. Safety of treatment, changes in risk factors, and incidence of coronary heart disease. *N. Engl. J. Med.* **317:** 1237–1245.
8. Meyers, C. D., V. S. Kamanna, and M. L. Kashyap. 2004. Niacin therapy in atherosclerosis. *Curr. Opin. Lipidol.* **15:** 659–665.
9. Rubins, H. B., S. J. Robins, D. Collins, C. L. Fye, J. W. Anderson, M. B. Elam, F. H. Faas, E. Linares, E. J. Schaefer, G. Schectman, et al. 1999. Gemfibrozil for the secondary prevention of coronary heart disease in men with low levels of high-density lipoprotein cholesterol. Veterans Affairs High-Density Lipoprotein Cholesterol Intervention Trial Study Group. *N. Engl. J. Med.* **341:** 410–418.
10. Davidson, M. H. 2008. Niacin use and cutaneous flushing: mechanisms and strategies for prevention. *Am. J. Cardiol.* **101:** 14B–19B.
11. Davidson, M. H., A. Armani, J. M. McKenney, and T. A. Jacobson. 2007. Safety considerations with fibrate therapy. *Am. J. Cardiol.* **99:** 3C–18C.
12. Rader, D. J. 2003. Effects of nonstatin lipid drug therapy on high-density lipoprotein metabolism. *Am. J. Cardiol.* **91:** 18E–23E.
13. Hooper, L., R. L. Thompson, R. A. Harrison, C. D. Summerbell, A. R. Ness, H. J. Moore, H. V. Worthington, P. N. Durrington, J. P. Higgins, N. E. Capps, et al. 2006. Risks and benefits of omega 3 fats for mortality, cardiovascular disease, and cancer: systematic review. *BMJ.* **332:** 752–760.
14. Kris-Etherton, P. M., W. S. Harris, and L. J. Appel. 2003. Fish consumption, fish oil, omega-3 fatty acids, and cardiovascular disease. *Arterioscler. Thromb. Vasc. Biol.* **23:** e20–e30.
15. Dastani, Z., J. C. Engert, J. Genest, and M. Marcil. 2006. Genetics of high-density lipoproteins. *Curr. Opin. Cardiol.* **21:** 329–335.
16. Wang, X., and B. Paigen. 2005. Genetics of variation in HDL cholesterol in humans and mice. *Circ. Res.* **96:** 27–42.
17. Kathiresan, S., A. K. Manning, S. Demissie, R. B. D'Agostino, A. Surti, C. Guiducci, L. Gianniny, N. P. Burtt, O. Melander, M. Orho-Melander, et al. 2007. A genome-wide association study for blood lipid phenotypes in the Framingham Heart Study. *BMC Med. Genet.* **8** (Suppl. 1): S17.
18. Willer, C. J., S. Sanna, A. U. Jackson, A. Scuteri, L. L. Bonnycastle, R. Clarke, S. C. Heath, N. J. Timpson, S. S. Najjar, H. M. Stringham, et al. 2008. Newly identified loci that influence lipid concentrations and risk of coronary artery disease. *Nat. Genet.* **40:** 161–169.
19. Deo, R. C., D. Reich, A. Tandon, E. Akylbekova, N. Patterson, A. Waliszewska, S. Kathiresan, D. Sarpong, H. A. Taylor, Jr., and J. G. Wilson. 2009. Genetic differences between the determinants of lipid profile phenotypes in African and European Americans: the Jackson Heart Study. *PLoS Genet.* **5:** e1000342.
20. Kathiresan, S., O. Melander, C. Guiducci, A. Surti, N. P. Burtt, M. J. Rieder, G. M. Cooper, C. Roos, B. F. Voight, A. S. Havulinna, et al. 2008. Six new loci associated with blood low-density lipoprotein cholesterol, high-density lipoprotein cholesterol or triglycerides in humans. *Nat. Genet.* **40:** 189–197.
21. Kathiresan, S., C. J. Willer, G. M. Peloso, S. Demissie, K. Musunuru, E. E. Schadt, L. Kaplan, D. Bennett, Y. Li, T. Tanaka, et al. 2009. Common variants at 30 loci contribute to polygenic dyslipidemia. *Nat. Genet.* **41:** 56–65.
22. Kooner, J. S., J. C. Chambers, C. A. Aguilar-Salinas, D. A. Hinds, C. L. Hyde, G. R. Warnes, F. J. Gomez Perez, K. A. Frazer, P. Elliott, J. Scott, et al. 2008. Genome-wide scan identifies variation in MLXIPL associated with plasma triglycerides. *Nat. Genet.* **40:** 149–151.
23. Lusis, A. J., and P. Pajukanta. 2008. A treasure trove for lipoprotein biology. *Nat. Genet.* **40:** 129–130.
24. Wallace, C., S. J. Newhouse, P. Braund, F. Zhang, M. Tobin, M. Falchi, K. Ahmadi, R. J. Dobson, A. C. Marcano, C. Hajat, et al. 2008. Genome-wide association study identifies genes for biomarkers of cardiovascular disease: serum urate and dyslipidemia. *Am. J. Hum. Genet.* **82:** 139–149.
25. Aulchenko, Y. S., S. Ripatti, I. Lindqvist, D. Boomsma, I. M. Heid, P. P. Pramstaller, B. W. Penninx, A. C. Janssens, J. F. Wilson, T. Spector, et al. 2009. Loci influencing lipid levels and coronary heart disease risk in 16 European population cohorts. *Nat. Genet.* **41:** 47–55.
26. Sabatti, C., S. K. Service, A. L. Hartikainen, A. Pouta, S. Ripatti, J. Brodsky, C. G. Jones, N. A. Zaitlen, T. Varilo, M. Kaakinen, et al. 2009. Genome-wide association analysis of metabolic traits in a birth cohort from a founder population. *Nat. Genet.* **41:** 35–46.
27. Rollins, J., Y. Chen, B. Paigen, and X. Wang. 2006. In search of new targets for plasma high-density lipoprotein cholesterol levels: promise of human-mouse comparative genomics. *Trends Cardiovasc. Med.* **16:** 220–234.
28. Stylianou, I. M., S. R. Langley, K. Walsh, Y. Chen, C. Revenu, and B. Paigen. 2008. Differences in DBA/1J and DBA/2J reveal lipid QTL genes. *J. Lipid Res.* **49:** 2402–2413.
29. DiPetrillo, K., X. Wang, I. M. Stylianou, and B. Paigen. 2005. Bioinformatics toolbox for narrowing rodent quantitative trait loci. *Trends Genet.* **21:** 683–692.
30. Sheehan, S., S. W. Tsaih, B. L. King, C. Stanton, G. A. Churchill, B. Paigen, and K. DiPetrillo. 2007. Genetic analysis of albuminuria in a cross between C57BL/6J and DBA/2J mice. *Am. J. Physiol. Renal Physiol.* **293:** F1649–F1656.
31. Reifsnyder, P. C., G. Churchill, and E. H. Leiter. 2000. Maternal environment and genotype interact to establish diabesity in mice. *Genome Res.* **10:** 1568–1578.
32. Su, Z., S. W. Tsaih, J. Szatkiewicz, Y. Shen, and B. Paigen. 2008. Candidate genes for plasma triglyceride, FFA, and glucose revealed from an intercross between inbred mouse strains NZB/B1NJ and NZW/LacJ. *J. Lipid Res.* **49:** 1500–1510.
33. Su, Z., R. Korstanje, S. W. Tsaih, and B. Paigen. 2008. Candidate genes for obesity revealed from a C57BL/6J x 129S1/SvImJ intercross. *Int. J. Obes. (Lond).* **32:** 1180–1189.
34. Churchill, G. A., and R. W. Doerge. 1994. Empirical threshold values for quantitative trait mapping. *Genetics.* **138:** 963–971.
35. Moran, J. L., A. D. Bolton, P. V. Tran, A. Brown, N. D. Dwyer, D. K. Manning, B. C. Bjork, C. Li, K. Montgomery, S. M. Siepka, et al. 2006. Utilization of a whole genome SNP panel for efficient genetic mapping in the mouse. *Genome Res.* **16:** 436–440.
36. Li, R., M. A. Lyons, H. Wittenburg, B. Paigen, and G. A. Churchill. 2005. Combining data from multiple inbred line crosses improves the power and resolution of quantitative trait loci mapping. *Genetics.* **169:** 1699–1709.
37. Frazer, K. A., E. Eskin, H. M. Kang, M. A. Bogue, D. A. Hinds, E. J. Beilharz, R. V. Gupta, J. Montgomery, M. M. Morenzoni, G. B. Nilsen, et al. 2007. A sequence-based variation map of 8.27 million SNPs in inbred mouse strains. *Nature.* **448:** 1050–1053.
38. Szatkiewicz, J. P., G. L. Beane, Y. Ding, L. Hutchins, F. Pardo-Manuel de Villena, and G. A. Churchill. 2008. An imputed genotype resource for the laboratory mouse. *Mamm. Genome.* **19:** 199–208.
39. Wiltshire, T., M. T. Pletcher, S. Batalov, S. W. Barnes, L. M. Tarantino, M. P. Cooke, H. Wu, K. Smylie, A. Santrosyan, N. G. Copeland, et al. 2003. Genome-wide single-nucleotide polymorphism analysis defines haplotype patterns in mouse. *Proc. Natl. Acad. Sci. USA.* **100:** 3380–3385.
40. Stylianou, I. M., J. P. Affourtit, K. R. Shockley, R. Y. Wilpan, F. A. Abdi, S. Bhardwaj, J. Rollins, G. A. Churchill, and B. Paigen. 2008. Applying gene expression, proteomics and single-nucleotide polymorphism analysis for complex trait gene identification. *Genetics.* **178:** 1795–1805.
41. Wang, X., R. Korstanje, D. Higgins, and B. Paigen. 2004. Haplotype analysis in multiple crosses to identify a QTL gene. *Genome Res.* **14:** 1767–1772.

42. Su, Z., A. Cox, Y. Shen, I. M. Stylianou, and B. Paigen. 2009. Farp2 and Stk25 are candidate genes for the HDL cholesterol locus on mouse chromosome 1. *Arterioscler. Thromb. Vasc. Biol.* **29:** 107–113.
43. Pan, H. J., Y. Lin, Y. E. Chen, D. E. Vance, and E. H. Leiter. 2006. Adverse hepatic and cardiac responses to rosiglitazone in a new mouse model of type 2 diabetes: relation to dysregulated phosphatidylcholine metabolism. *Vascul. Pharmacol.* **45:** 65–71.
44. Colinayo, V. V., J. H. Qiao, X. Wang, K. L. Krass, E. Schadt, A. J. Lusis, and T. A. Drake. 2003. Genetic loci for diet-induced atherosclerotic lesions and plasma lipids in mice. *Mamm. Genome.* **14:** 464–471.
45. Nadeau, J. H. 2001. Modifier genes in mice and humans. *Nat. Rev. Genet.* **2:** 165–174.
46. Kullo, I. J., S. T. Turner, E. Boerwinkle, S. L. Kardia, and M. de Andrade. 2005. A novel quantitative trait locus on chromosome 1 with pleiotropic effects on HDL-cholesterol and LDL particle size in hypertensive sibships. *Am. J. Hypertens.* **18:** 1084–1090.
47. Mural, R. J., M. D. Adams, E. W. Myers, H. O. Smith, G. L. Miklos, R. Wides, A. Halpern, P. W. Li, G. G. Sutton, J. Nadeau, et al. 2002. A comparison of whole-genome shotgun-derived mouse chromosome 16 and the human genome. *Science.* **296:** 1661–1671.
48. Mackay, T. F. 2001. The genetic architecture of quantitative traits. *Annu. Rev. Genet.* **35:** 303–339.
49. Yalcin, B., S. A. Willis-Owen, J. Fullerton, A. Meesaq, R. M. Deacon, J. N. Rawlins, R. R. Copley, A. P. Morris, J. Flint, and R. Mott. 2004. Genetic dissection of a behavioral quantitative trait locus shows that Rgs2 modulates anxiety in mice. *Nat. Genet.* **36:** 1197–1202.
50. Hawley, R. S., and W. D. Gilliland. 2006. Sometimes the result is not the answer: the truths and the lies that come from using the complementation test. *Genetics.* **174:** 5–15.
51. Ma, K., M. Cilingiroglu, J. D. Otvos, C. M. Ballantyne, A. J. Marian, and L. Chan. 2003. Endothelial lipase is a major genetic determinant for high-density lipoprotein concentration, structure, and metabolism. *Proc. Natl. Acad. Sci. USA.* **100:** 2748–2753.
52. Su, Z., X. Wang, S. W. Tsaih, A. Zhang, A. Cox, S. Sheehan, and B. Paigen. 2009. Genetic basis of HDL variation in 129/SvImJ and C57BL/6J mice: importance of testing candidate genes in targeted mutant mice. *J. Lipid Res.* **50:** 116–125.
53. Darvasi, A. 1997. Interval-specific congenic strains (ISCS): an experimental design for mapping a QTL into a 1-centimorgan interval. *Mamm. Genome.* **8:** 163–167.
54. Gale, G. D., R. D. Yazdi, A. H. Khan, A. J. Lusis, R. C. Davis, and D. J. Smith. 2008. A genome-wide panel of congenic mice reveals widespread epistasis of behavior quantitative trait loci. *Mol. Psychiatry.* **14:** 631–645.
55. Stylianou, I. M., S. W. Tsaih, K. DiPetrillo, N. Ishimori, R. Li, B. Paigen, and G. Churchill. 2006. Complex genetic architecture revealed by analysis of high-density lipoprotein cholesterol in chromosome substitution strains and F2 crosses. *Genetics.* **174:** 999–1007.
56. Rankinen, T., A. Zuberi, Y. C. Chagnon, S. J. Weisnagel, G. Argyropoulos, B. Walts, L. Perusse, and C. Bouchard. 2006. The human obesity gene map: the 2005 update. *Obesity (Silver Spring).* **14:** 529–644.
57. Wang, X., N. Ishimori, R. Korstanje, J. Rollins, and B. Paigen. 2005. Identifying novel genes for atherosclerosis through mouse-human comparative genetics. *Am. J. Hum. Genet.* **77:** 1–15.
58. Maugeais, C., U. J. Tietge, U. C. Broedl, D. Marchadier, W. Cain, M. G. McCoy, S. Lund-Katz, J. M. Glick, and D. J. Rader. 2003. Dose-dependent acceleration of high-density lipoprotein catabolism by endothelial lipase. *Circulation.* **108:** 2121–2126.
59. Ishida, T., S. Choi, R. K. Kundu, K. Hirata, E. M. Rubin, A. D. Cooper, and T. Quertermous. 2003. Endothelial lipase is a major determinant of HDL level. *J. Clin. Invest.* **111:** 347–355.
60. Bosse, Y., Y. C. Chagnon, J. P. Despres, T. Rice, D. C. Rao, C. Bouchard, L. Perusse, and M. C. Vohl. 2004. Compendium of genome-wide scans of lipid-related phenotypes: adding a new genome-wide search of apolipoprotein levels. *J. Lipid Res.* **45:** 2174–2184.
61. Jahangiri, A., D. J. Rader, D. Marchadier, L. K. Curtiss, D. J. Bonnet, and K. A. Rye. 2005. Evidence that endothelial lipase remodels high density lipoproteins without mediating the dissociation of apolipoprotein A-I. *J. Lipid Res.* **46:** 896–903.
62. Hutter, C. M., M. A. Austin, F. M. Farin, H. M. Viernes, K. L. Edwards, D. L. Leonetti, M. J. McNeely, and W. Y. Fujimoto. 2006. Association of endothelial lipase gene (LIPG) haplotypes with high-density lipoprotein cholesterol subfractions and apolipoprotein AI plasma levels in Japanese Americans. *Atherosclerosis.* **185:** 78–86.
63. Mank-Seymour, A. R., K. L. Durham, J. F. Thompson, A. B. Seymour, and P. M. Milos. 2004. Association between single-nucleotide polymorphisms in the endothelial lipase (LIPG) gene and high-density lipoprotein cholesterol levels. *Biochim. Biophys. Acta.* **1636:** 40–46.
64. Edmondson, A. C., R. J. Brown, S. Kathiresan, L. A. Cupples, S. Demissie, A. K. Manning, M. K. Jensen, E. B. Rimm, J. Wang, A. Rodrigues, et al. 2009. Loss-of-function variants in endothelial lipase are a cause of elevated HDL cholesterol in humans. *J. Clin. Invest.* **119:** 1042–1050.
65. Wergedal, J. E., C. L. Ackert-Bicknell, W. G. Beamer, S. Mohan, D. J. Baylink, and A. K. Srivastava. 2007. Mapping genetic loci that regulate lipid levels in a NZB/B1NJxRF/J intercross and a combined intercross involving NZB/B1NJ, RF/J, MRL/MpJ, and SJL/J mouse strains. *J. Lipid Res.* **48:** 1724–1734.
66. Brockmann, G. A., E. Karatayli, C. Neuschl, I. M. Stylianou, S. Aksu, A. Ludwig, U. Renne, C. S. Haley, and S. Knott. 2007. Genetic control of lipids in the mouse cross DU6i x DBA/2. *Mamm. Genome.* **18:** 757–766.
67. Wang, S. S., W. Shi, X. Wang, L. Velky, S. Greenlee, M. T. Wang, T. A. Drake, and A. J. Lusis. 2007. Mapping, genetic isolation, and characterization of genetic loci that determine resistance to atherosclerosis in C3H mice. *Arterioscler. Thromb. Vasc. Biol.* **27:** 2671–2676.
68. Machleder, D., B. Ivandic, C. Welch, L. Castellani, K. Reue, and A. J. Lusis. 1997. Complex genetic control of HDL levels in mice in response to an atherogenic diet. Coordinate regulation of HDL levels and bile acid metabolism. *J. Clin. Invest.* **99:** 1406–1419.
69. Mehrabian, M., L. W. Castellani, P. Z. Wen, J. Wong, T. Rithaporn, S. Y. Hama, G. P. Hough, D. Johnson, J. J. Albers, G. A. Mottino, et al. 2000. Genetic control of HDL levels and composition in an interspecific mouse cross (CAST/Ei x C57BL/6J). *J. Lipid Res.* **41:** 1936–1946.
70. Korstanje, R., R. Li, T. Howard, P. Kelmenson, J. Marshall, B. Paigen, and G. Churchill. 2004. Influence of sex and diet on quantitative trait loci for HDL cholesterol levels in an SM/J by NZB/BlNJ intercross population. *J. Lipid Res.* **45:** 881–888.